

Quasi-binary amorphous phase in a 3D system of particles with repulsive-shoulder interactions

Yu. D. Fomin, N. V. Gribova, V. N. Ryzhov, and S. M. Stishov

Institute for High Pressure Physics, Russian Academy of Sciences, Troitsk 142190, Moscow Region, Russia

Daan Frenkel

FOM Institute for Atomic and Molecular Physics, Amsterdam,

The Netherlands and Dept. of Chemistry, Univ. of Cambridge, Cambridge, UK

(Dated: February 9, 2022)

We report a computer-simulation study of the equilibrium phase diagram of a three-dimensional system of particles with a repulsive step potential. Using free-energy calculations, we have determined the equilibrium phase diagram of this system. At low temperatures, we observe a number of distinct crystal phases. However, under certain conditions the system undergoes a glass transition in a regime where the liquid appears thermodynamically stable. We argue that the appearance of this amorphous low-temperature phase can be understood by viewing this one-component system as a pseudo-binary mixture.

PACS numbers: 61.20.Gy, 61.20.Ne, 64.60.Kw

Many ordered materials can undergo a first-order phase transition that does not alter the symmetry of the phase. In the early work of Hemmer and Stell [1] it was proposed that such iso-structural phase transitions are to be expected if the interaction between the particles in addition to the ordinary hard core has a “soft” core combined with an attractive interaction at larger distances. The work of ref. [1] focused specifically on iso-structural phase transitions in materials such as Ce or Cs, but since then many authors have studied a wide range of model system that could exhibit iso-structural transitions [2, 3, 4, 5, 6, 7, 8, 9, 10, 11, 12]. Most of these systems have a repulsive intermolecular potential that has a region of negative curvature, a feature that is known to be present in the interatomic potentials of some pure metallic systems, metallic mixtures, electrolytes and colloidal systems. The simplest example of a negative-curvature potential is the repulsive-step potential which consists of a hard core plus a finite repulsive shoulder at a larger radius. Systems of particles interacting through such pair potentials can possess a rich variety of phase transitions and thermodynamic anomalies, including liquid-liquid phase transitions [5, 6], water-like anomalies [7], and isostructural transitions in the solid region [10, 11].

The repulsive step potential has the form:

$$\Phi(r) = \begin{cases} \infty, & r \leq d \\ \varepsilon, & d < r \leq \sigma \\ 0, & r > \sigma \end{cases} \quad (1)$$

where d is the diameter of the hard core, σ is the width of the repulsive step, and ε its height. In the low-temperature limit $\tilde{T} \equiv k_B T / \varepsilon \ll 1$ the system reduces to a hard-sphere systems with hard-sphere diameter σ , whilst in the limit $\tilde{T} \gg 1$ the system reduces to a hard-sphere model with a hard-sphere diameter d . For this reason, melting at high and low temperatures follows

simply from the hard-sphere melting curve $P = cT/\sigma'^3$, where $c \approx 12$ and σ' is the relevant hard-sphere diameter (σ and d , respectively). A changeover from the low- T to high- T melting behavior should occur for $\tilde{T} = \mathcal{O}(1)$. The precise form of the phase diagram depends on the ratio $s \equiv \sigma/d$. For large enough values of s one should expect to observe in the resulting melting curve a maximum that should disappear as $s \rightarrow 1$ [12]. The phase behavior in the crossover region may be very complex, as shown below.

In our simulations we have used a smoothed version of the repulsive step potential (Eqn. 1), which has the form:

$$\Phi(r) = \left(\frac{d}{r}\right)^n + \frac{1}{2}\varepsilon(1 - \tanh(k_0(r - \sigma_s))) \quad (2)$$

where $n = 14$, $k_0 = 10$. We have considered the following values of σ_s : $\sigma_s = 1.15, 1.35$. In the remainder of this paper we use the dimensionless quantities: $\tilde{\mathbf{r}} \equiv \mathbf{r}/d$, $\tilde{P} \equiv Pd^3/\varepsilon$, $\tilde{V} \equiv V/Nd^3 \equiv 1/\tilde{\rho}$. As we will only use these reduced variables, we omit the tildes.

In order to get a hint about the phase diagrams of the system we computed energies per particle for different crystal ground states for $\sigma_s = 1.15, 1.35$. In the upper part of Fig. 1 we plot a schematic phase diagram at $T = 0$ for $\sigma_s = 1.15$. It is obtained from the calculation of the ground state energy of the FCC (face-centered cubic) and BCC (body-centered cubic) crystal structures. We also considered several other structures for this potential - SC (simple cubic), HCP, diamond structure, FCO (face-centered orthorhombic) and BCO (body-centered orthorhombic) but all these were unstable.

In the lower part of Fig. 1 we show the schematic phase diagram at $T = 0$ for $\sigma_s = 1.15$. It is plotted from the calculation of the ground state energies of the FCC, BCC, SC, diamond and FCO structures for $\sigma_s = 1.35$. Fig. 1 shows that there exists a range of densities where

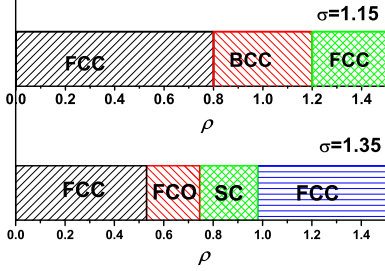


FIG. 1: Ground state. The schematic phase diagrams at $T = 0$ for $\sigma_s = 1.15$ and $\sigma_s = 1.35$.

the stable phase has an FCO structure whose unit cell is increased along the z axis in 1.6 times. This is a clear indication that the phase diagrams in the solid region are quite complex.

To determine the phase diagram at non-zero temperature, we performed constant-NVT MD simulations combined with free-energy calculations. In all cases, periodic boundary conditions were used. The number of particles varied between 250 and 500. No system-size dependence of the results was observed. The system was equilibrated for 5×10^6 MD time steps. Data were subsequently collected during $3 \times 10^6 \delta t$ where the time step $\delta t = 5 \times 10^{-5}$.

In some region of the phase diagram for $\sigma_s = 1.35$ we found that the liquid phase was thermodynamically stable down to the lowest temperatures that we could probe. In this region of the phase diagram, the dynamics of the system was very sluggish, forcing us to perform much longer MD simulations (up to 90×10^6 MD steps).

In order to map out the phase diagram of the system, we computed its Helmholtz free energy using the thermodynamic integration: the free energy of the liquid phase was computed via thermodynamic integration from the dilute gas limit [13], and the free energy of the solid phase was computed by thermodynamic integration to an Einstein crystal [13, 14]. In the MC simulations of solid phases, data were collected during 5×10^4 cycles after equilibration. To improve the statistics (and to check for internal consistency) the free energy of the solid was computed at many dozens of different state-points. All free-energy data were used to construct a single multinomial fit for the equation of state in every phase. The transition points were determined by a double-tangent construction (DTC).

Fig. 2 shows the phase diagrams that we obtain from the free-energy calculations for two different values of σ_s . Figs. 2(a-b) show the phase diagram of the system with $\sigma_s = 1.15$. One can see that for the system with $\sigma_s = 1.15$ there are no maxima in the melting curve. In a soft-sphere system described by the potential

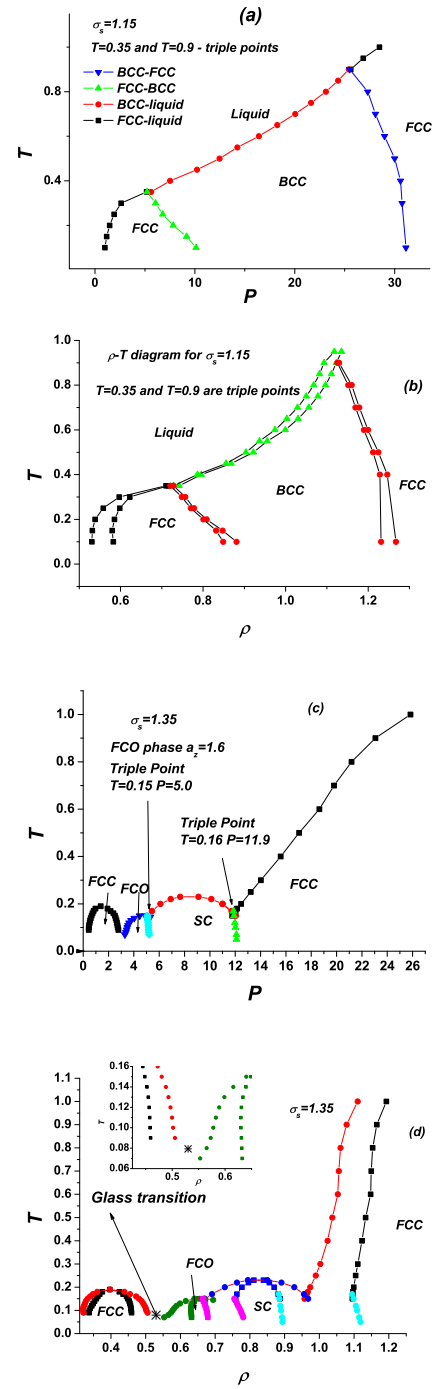


FIG. 2: Phase diagram of the system of particles interacting through the potential (2) with $\sigma_s = 1.15, 1.35$ in $P - T$ and $\rho - T$ planes. The asterisk in Fig. (d) corresponds to the glass transition.

$1/r^{14}$ a face-centered cubic crystal structure has been reported [15]. However, the addition of a small repulsive step leads to the appearance of the FCC-BCC transition shown in Figs. 2(a-b).

Figs. 2(c-d) show the phase diagram of the system with

$\sigma_s = 1.35$ in the $P-T$ and $\rho-T$ planes. There is a clear maximum in the melting curve at low densities. The phase diagram consists in two isostructural FCC parts corresponding to close packing of the small and large spheres separated by a sequence of structural phase transitions.

This complexity of the phase diagram can be understood from the shape of the potential. Since the potential is purely repulsive, the particles tend to minimize both hard and soft-core overlaps. Such overlaps can be avoided in the low pressure part of the phase diagram. Upon increasing the density, the system crystallizes into FCC phase which corresponds to the close packing of the particles at the soft core. If the pressure increases more, the particles begin to penetrate the soft core but still avoid hard-core overlaps. Hence, both parts of the potential are now important. The FCO phase corresponds to the situation when the particles are packed in $X-Y$ planes in accordance with the hard core but the planes are arranged at the soft core distance (layered structure). As a result a particle has 4 nearest neighbors in this structure. If we further increase the pressure, more particles penetrate the soft core, but still the closed packed structures are not favorable. Finally at very high pressures region we observe the FCC phase corresponding to the r^{-14} limit.

Interestingly, there is a region of the phase diagram where we have not found any stable crystal phase. In order to clarify the properties of the system in the "gap" on the phase diagram between the low-density FCC phase and FCO phase, we compute mean-squared displacement (MSD, $\Delta r^2(t)$) and self-correlation function $F_s(q, t)$ for different temperatures at $\rho = 0.53$ (Fig. 3). As usually observed in the proximity of liquid-glass transition [16, 17, 18], a bending occurs in the MSD after the initial ballistic regime (Fig. 3(a)). A plateau appears at low temperatures which corresponds to the onset of the caging regime. At long time, the diffusion regime ($\Delta r^2(t) \propto t$) is reached, when the particles move, on average, a distance of the order of their size.

Another plateau is observed for self-correlation function $F_s(q, t)$ (Fig. 3(b)) in the time interval corresponding to the caging regime (β -relaxation regime in mode-coupling theory [19, 20, 21]). The correlation functions start to decay from the plateau at times corresponding to the onset of the diffusive regime in the MSD (α -relaxation regime). In order to estimate the transition temperature, we calculate diffusivity D as the long time limit of $\langle \Delta r(t)^2 \rangle / 6t$. As predicted by Mode-Coupling Theory (MCT), in the vicinity of a glass transition point there is the power-law temperature dependence of the diffusivity $D \propto (T - T_c)^\gamma$. In accordance with MCT [19, 20, 21], $\gamma \geq 1.75$. From Fig. 3(a) one has $T_c = 0.079$ and $\gamma = 2.29$.

The apparent glass-transition temperature is above the melting point of the low-density FCC and FCO phases

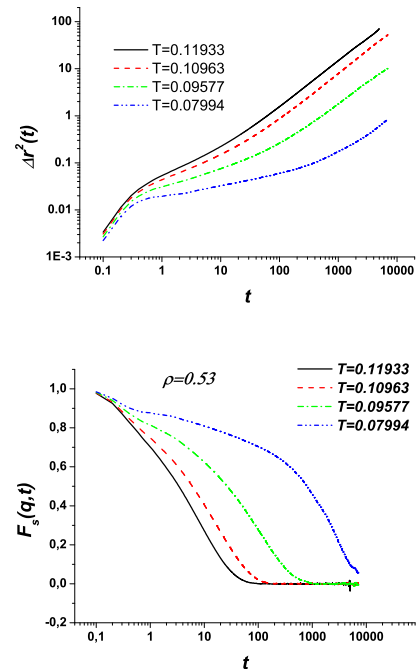


FIG. 3: (a) MSD and (b) self-correlation function $F_s(q, t)$ as functions of time for $\sigma = 1.35$ for different temperatures at $\rho = 0.53$.

(see Fig. 2(d)). This suggests that the "glassy" phase that we observe is thermodynamically stable. This is rather unusual for one-component liquids. In simulations, glassy behavior is usually observed in metastable mixtures (see e.g. [16, 17, 18]) where crystal nucleation is kinetically suppressed. One could argue that, in the glassy region, the present system behaves like a "pseudo-binary" mixture of spheres with diameters d and σ_s and that the freezing-point depression is analogous to that expected in a binary system with a eutectic point: there are some values of the diameter ratio such that crystalline structures are strongly unfavorable and the glassy phase is stable even for very low temperatures. The glassy behavior in the reentrant liquid disappears at higher temperatures. In this density range we also found the anomalous behavior of isochores which corresponds to the negative thermal expansion coefficient. This behavior will be discussed in detail in a subsequent publication.

The behavior that we observe in this three-dimensional system bears some striking similarities to that observed in two-dimensional system with "repulsive-shoulder" potentials [22, 23, 24, 25]. These simulations suggest that such systems have a low-temperature reentrant liquid phase where particles intend to arrange in more or less complex, locally ordered patterns. Norizoe and Kawakatsu [25] find evidence for local clustering and the formation of percolating clusters in the reentrant liquid phase of a 3D repulsive-shoulder model. Moreover,

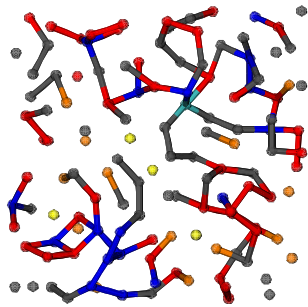


FIG. 4: (Color online). Snapshot of the disordered phase for the $\sigma_s = 1.35$, for $\rho = 0.55$, $T = 0.1$. The colors on the snapshots correspond to the number of the nearest neighbours (yellow - 0, orange - 1, dark grey - 2, red - 3, blue - 4, light blue - 5).

refs. [22, 23, 24, 25] find that diffusion in this part of the phase diagram is very slow - for this reason, they refer to these percolating cluster phases as “amorphous solids”. However, none of these studies include free-energy calculations and hence the equilibrium phase boundaries between solid and reentrant liquid are not known. Our free energy calculations support that the notion that these amorphous solids are thermodynamically stable.

In the Fig. 4 we represent the snapshot of our system in this region for $\sigma_s = 1.35$, for $\rho = 0.55$, $T = 0.1$. Particles in the snapshot are colored according to the number of the nearest neighbours. The nearest neighbours to the particle X were considered to be all particles within the distance of the first minimum of the radial distribution function. After reentrant melting the structure corresponds to an assembly of linear “strings” of particles with 2 near neighbours. It is possible that the structure of liquid here is 3D analog of the spatial configurations found in [23], this point clearly requires further study.

In summary, we have performed the extensive computer simulations of the phase behavior of systems described by the soft, purely repulsive step potential (2) in three dimensions. We find a surprisingly complex phase behavior. We argue that the evolution of the phase diagram may be qualitatively understood by considering this one-component system as a pseudo-binary mixture of large and small spheres. Interestingly, the phase diagram includes two crystalline FCC domains separated by a sequence of the structural phase transitions and a reentrant liquid that becomes amorphous at low temperatures. The phase behavior of systems with even wider repulsive steps will be discussed in separate publication.

We thank V. V. Brazhkin for stimulating discussions. The work was supported in part by the Russian Foundation for Basic Research (Grants No 05-02-17280 and No 05-02-17621), the Fund of the President of Russian Federation for Support of Young Scientists (MK-2905.2007.2) and NWO-RFBR Grant No 047.016.001. The work of the FOM Institute is part of the research program of FOM and is made possible by financial support from the

Netherlands organization for Scientific Research (NWO).

-
- [1] P. C. Hemmer and G. Stell, Phys. Rev. Lett. **24**, 1284(1970); G. Stell and P. C. Hemmer, J. Chem. Phys. **56**, 4274 (1972).
 - [2] V. V. Brazhkin, S. V. Buldyrev, V. N. Ryzhov, and H. E. Stanley [eds], *New Kinds of Phase Transitions: Transformations in Disordered Substances* [Proc. NATO Advanced Research Workshop, Volga River] (Kluwer, Dordrecht, 2002).
 - [3] G. Malescio, J. Phys.: Condens. Matter **19**, 07310 (2007).
 - [4] E. Velasco, L. Mederos, G. Navascues, P. C. Hemmer, and G. Stell, Phys. Rev. Lett. **85**, 122 (2000); P. C. Hemmer, E. Velasco, L. Mederos, G. Navascues, and G. Stell, J. Chem. Phys. **114**, 2268 (2001).
 - [5] V. N. Ryzhov and S. M. Stishov, Zh. Eksp. Teor. Fiz. **122**, 820 (2002)[JETP **95**, 710 (2002)]; V. N. Ryzhov and S. M. Stishov, Phys. Rev. E **67**, 010201(R) (2003).
 - [6] Yu. D. Fomin, V. N. Ryzhov, and E. E. Tareyeva, Phys. Rev. E **74**, 041201 (2006).
 - [7] M. R. Sadr-Lahijany, A. Scala, S. V. Buldyrev and H. E. Stanley, Phys. Rev. Lett. **81**, 4895 (1998).
 - [8] M. R. Sadr-Lahijany, A. Scala, S. V. Buldyrev and H. E. Stanley, Phys. Rev. E **60**, 6714 (1999); P. Kumar, S. V. Buldyrev, F. Sciortino, E. Zaccarelli, and H. E. Stanley, Phys. Rev. E **72**, 021501 (2005); L. Xu, S. V. Buldyrev, C. A. Angell, and H. E. Stanley, Phys. Rev. E **74**, 031108 (2006).
 - [9] E. A. Jagla, J. Chem. Phys. **111**, 8980 (1999); E. A. Jagla, Phys. Rev. E **63**, 061501 (2001).
 - [10] D. A. Young and B. J. Alder, Phys. Rev. Lett. **38**, 1213 (1977); D. A. Young and B. J. Alder, J. Chem. Phys. **70**, 473 (1979).
 - [11] P. Bolhuis and D. Frenkel, J. Phys.: Condens. Matter **9**, 381 (1997).
 - [12] S. M. Stishov, Phil. Mag. B **82**, 1287 (2002).
 - [13] Daan Frenkel and Berend Smit, *Understanding molecular simulation (From Algorithms to Applications)*, 2nd Edition (Academic Press), 2002.
 - [14] D. Frenkel and A. J. Ladd, J. Chem. Phys. **81**, 3188 (1984).
 - [15] R. Agrawal and D.A. Kofke, Phys. Rev. Lett. **74**, 122 (1995).
 - [16] W. Kob and H.C. Andersen, Phys. Rev. Lett. **73**, 1376 (1994); Phys. Rev. E **51**, 4626 (1995); Phys. Rev. E **52**, 4134 (1995).
 - [17] W. Kob, J. Phys.: Condens. Matter **11**, R85 (1999).
 - [18] A.J. Moreno and J. Colmenero, J. Chem. Phys. **125**, 164507 (2006).
 - [19] W. Gotze and L. Sjorgen, Rep. Prog. Phys. **55**, 241 (1992).
 - [20] W. Gotze, J. Phys.: Condens. Matter **11**, A1 (1999)
 - [21] S.P. Das, Rev. Mod. Phys. **76**, 785 (2004).
 - [22] P.J. Camp, Phys. Rev. E **68**, 061506 (2003).
 - [23] G. Malescio and G. Pellicane, Phys. Rev. E **70**, 021202 (2004).
 - [24] M.A. Glaser et al., arXiv:cond-mat/0609570.
 - [25] Y. Norizoe and T. Kawakatsu, Europhys. Lett., **72**,583 (2005).